Journal of Power Sources 193 (2009) 585–588

Contents lists available at ScienceDirect

Journal of Power Sources

journal homepage: www.elsevier.com/locate/jpowsour

Short communication

# A long-term degradation study of power generation characteristics of anode-supported solid oxide fuel cells using LaNi(Fe)$O_3$ electrode

Takeshi Komatsu*, Kimitaka Watanabe, Masayasu Arakawa, Hajime Arai

*NTT Corporation, NTT Energy and Environment Systems Laboratories, Morinosato-Wakamiya 3-1, Atsugi-shi, Kanagawa 243-0198, Japan*

ARTICLE INFO

*Article history:*
Received 18 November 2008
Received in revised form 9 March 2009
Accepted 14 April 2009
Available online 22 April 2009

*Keywords:*
SOFC
Fuel cells
LNF
Degradation

ABSTRACT

The long-term operation of an anode-supported solid oxide fuel cell was examined to study the degradation factor. The cell was constructed using $LaNi_{0.6}Fe_{0.4}O_3$ (LNF), alumina-doped scandia stabilized zirconia (SASZ), and NiO-SASZ as the cathode, electrolyte, and anode respectively. The cell had Pt current collectors and was operated for 6500 h. The test was carried out at 1073 K with a constant load of 0.4 A $cm^{-2}$ and included thermal cycling. The cell voltage degradation rate was below 0.86%/1000 h when the cell was operated for up to 5200 h. Changes in the resistance of the cells during the experiments were analyzed by impedance spectroscopy. The cathode polarization resistance and ohmic resistance increased with time. The elements (Si and B) contained in the water condensed from the cathode exhaust gas were identified using inductively coupled plasma (ICP).



## 1. Introduction

Solid oxide fuel cells (SOFCs) have the potential to provide electrical power with high efficiency and a low environmental impact [1,2]. SOFCs have high operating temperatures (around 1273 K) and require the use of the specific ceramic materials as seals and interconnect. However, the development of intermediate temperature (below 1273 K) SOFCs could extend cell lifetimes, making it possible to use inexpensive metal components as interconnects and reduce fabrication costs. Moreover, metal interconnects have the advantages of ease of handling and sufficient mechanical strength. However, if intermediate temperature SOFCs are to be used in practice, it is necessary to develop electrode materials that are active at low operating temperature of about 1073 K.

We have used LaNi(Fe)$O_3$ (LNF) cathode for anode-supported cells because LNF has high electronic conductivity [3], a thermal expansion coefficient that matches that of zirconia electrolyte [3], and a high tolerance to Cr poisoning [4–6]. We have already confirmed that 60-mm Φ cells with LNF cathode using Pt current collectors can achieve a high power density of 1.6 W $cm^{-1}$ [2,7]. We have tested the long-term stability of a cell with a Pt current collector for 6000 h [8]. The degradation rate was 0.4%/1000 h. A 25-cell stack was developed by using anode-supported planar 100-mm Φ cells with metallic interconnects [9]. When reformed methane was supplied to the stack, we obtained an electrical power output of 350 W and a conversion efficiency of 56% at a current density of 0.3 A $cm^{-2}$ and a fuel utilization rate of 75%. The efficiency stayed constant for over 1000 h. A 50-cell stack with 120-mm Φ cells exhibited an electrical power output of 1.1 kW and a conversion efficiency of 54% at a current density of 0.3 A $cm^{-2}$ when the reformed methane utilization rate was 67% [10]. However, the reliability of this cell after several thousand hours has not yet been studied in detail.

Some groups have tested the long-term operation of cells, stacks and SOFC systems [11,12]. The Kansai Electric Power Co. Inc. and Mitsubishi Materials Corporation have been developing a 10 kW-class stack module with an electrical efficiency of over 40% HHV. The accumulated operating time was about 2500 h [11]. The Tokyo Gas Co. conducted cell durability tests as a function of the elapsed time and the thermal cycle [12]. The cell operated stably at 0.2 A $cm^{-2}$ and 1048 K for over 4000 h. The cell voltage degradation rate was 0.28%/1000 h. Other groups have studied the cell and stacks degradation factors [13,14]. Horita et al. investigated the durability of a 20-cells stack [13]. The experiment was conducted at 1023 K with dry $H_2$ under a constant current density of 0.3 A $cm^{-2}$ for more than 5000 h. Some impurities (Na, Al, Si, and Cr) were detected at the cathode and the cathode–electrolyte interlayer by SIMS after the long-term operation test. Haga et al. evaluated the influence of various fuel impurities, including sulfur compounds, chlorine, and siloxane, on anode performance [14]. The cell voltage degradation rate increased with increasing impurity concentration. They also suggested degradation mechanism for each impurity. There are various factors that influence the degradation and these have not yet been clarified.

We also clarify possible degradation factors with a view to improve cell lifetime. This paper reports a long-term degradation

* Corresponding author. Tel.: +81 46 240 2532; fax: +81 46 270 2702.
*E-mail address:* takeshi@aecl.ntt.co.jp (T. Komatsu).

0378-7753/$ – see front matter © 2009 Elsevier B.V. All rights reserved.
doi:10.1016/j.jpowsour.2009.04.014

study of the power generation characteristics of anode-supported solid oxide fuel cells using a $LaNi(Fe)O_3$ electrode.

## 2. Experimental

### 2.1. Cell fabrication

An anode-supported cell (60 mm Φ) was fabricated by the co-firing method, which is described elsewhere in detail [7,8,15]. SASZ (10 mol.% $Sc_2O_3$- and 1 mol.% $Al_2O_3$-stabilized $ZrO_2$) electrolyte paste on an anode green sheet was screen-printed and co-sintered, followed by the screen printing and firing of the cathode. The anode substrate was made of Ni-SASZ. LNF ($LaNi_{0.6}Fe_{0.4}O_3$) was used as the cathode material. A LNF-SDC ($Sm_{0.2}Ce_{0.8}O_{19}$) interlayer was inserted between the electrolyte and cathode [16].

### 2.2. Electrochemical measurement

As shown in Fig. 1, we performed a test employing an alumina test housing with current collectors, for which we used a Pt mesh with ceramic paste at the cathode and Pt mesh with Pt paste at the anode. Commercial borosilicate glass was used to join the ceramic cell and metal interconnect. A long-term test was carried out at 1073 K with a constant load of 0.4 A $cm^{-2}$ (electrode area: 19.6 $cm^2$). About 3% humidified hydrogen gas was used as the fuel on the anode side with a flow rate of 500 sccm. Dry air ($P_{H_2O}$ : $1 \times 10^{-7}$ atm) was used as the oxidant at a flow rate of 800 sccm. During the test, the cell was thermally cycled twice between room temperature and 1073 K. The current–voltage curves and impedances were measured intermittently. AC impedance measurements were performed over the frequency range of 0.01 Hz to 63 kHz frequency range with an amplitude of 10 mV by using the four-terminal method at 1073 K in the vicinity of the open circuit voltage (OCV). For this measurement, we used a frequency analyzer (Solatron 1250) and a potentiostat (Solatron SI1287).

### 2.3. Characterization

The water vapor contained in the cathode exhaust gas during the power generation test was condensed at room temperature. Water samples were collected from the condenser at intervals of several hundred hours, and the elements in the water were identified by using inductively coupled plasma (ICP, IRIS/AP HR Advantage, Thermo-Jarrell Ash).

## 3. Results and discussion

The time dependence of the cell voltage during long-term operation is shown in Fig. 2. The current–voltage ($I$–$V$) curves and impedance spectra were measured for states 1–6 shown in Table 1. There was a slight decrease in the cell voltage during 5200 h operation at 0.4 A $cm^{-2}$ and 1073 K. A slight increase in the cell voltage was observed during the initial 1000 h operation. We think that this gradual improvement in the performance can be attributed to the sintering of the cathode during the current loading process [16,17], which resulted in a reduction in the interface resistance and ohmic resistance after the current had been loaded. We defined the cell voltage degradation rate using the follow formula. The initial voltage and the voltage measured at an arbitrary operating time are expressed as $V_0$ and $V_t$, respectively.

$$\text{Cell voltage degradation rate}\,(\%) = \frac{V_0 - V_t}{V_0} \times 100$$

The voltage degradation rate was 0.86%/1000 h during the operation that included the first thermal cycle between 0 and 5200 h. After the second thermal cycle, the voltage drastically decreased greatly. The voltage degradation rate was 1.40%/1000 h during operation between 0 and 5670 h.

Fig. 3 shows the $I$–$V$ characteristics of the cell measured for states 1–6. The $I$–$V$ characteristics degraded in accordance with the voltage behavior during the constant current operation shown in Fig. 2. The initial OCV for state 1 was 1.10 V, which exactly matched the theoretical (Nernst) voltage (anode: $H_2$ + 3 vol.% $H_2O$; cathode: dry air) at 1073 K. After 2300 h, the OCV value for state 2 was similar to that for state 1, which shows that the gas seal remained intact during the power generation test. Before and after the first thermal cycle, the OCV fell from 1.10 to 1.08 V. After that, it remained a constant value for a period ranging from 5200 to 5670 h. After the second thermal cycle, it decreased to about 1.07 V. This OCV drop is probably due to a gas leak from the anode side.

The impedance spectrum was measured to clarify the reason for the measured degradation of the cell. Fig. 4 shows a typical impedance spectrum, which was measured for state 1. There are two arcs: one with a high frequency and the other with a low frequency. In our measurements, we found that the size for a

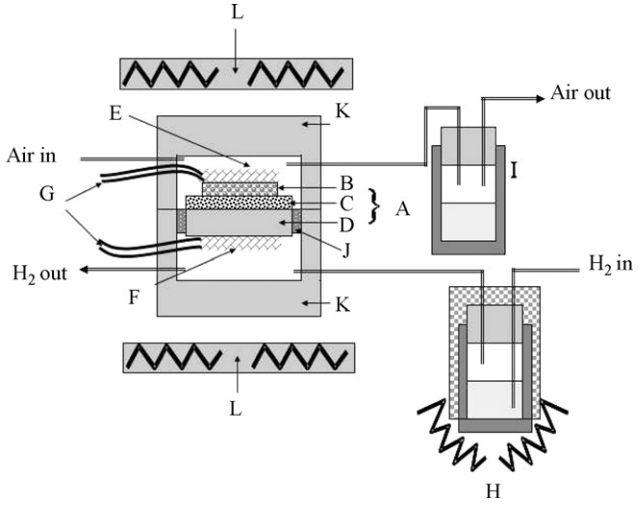


**Fig. 1.** Testing equipment: (A) cell; (B) cathode; (C) electrolyte; (D) anode; (E) cathode current collector (Pt mesh and ceramic paste); (F) anode current collector (Pt mesh and Pt paste); (G) current and voltage lead (Pt wire); (H) bubbler; (I) condenser (cathode exhaust gas); (J) glass sealant; (K) alumina housing; (L) heater.

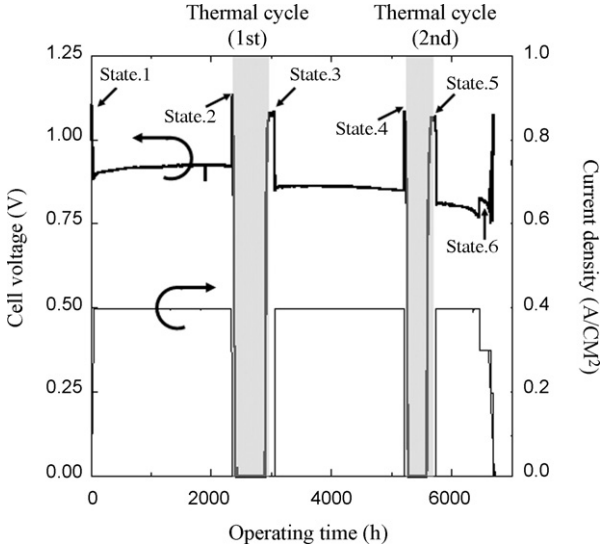


**Fig. 2.** Cell voltage as a function of operating time.

**Table 1**
Electrochemical performance of the cell for states 1–6.

| | Operation time (h) | Cell voltage at 0 A cm$^{-2}$ (V) | Cell voltage at 0.4 A cm$^{-2}$ (V) | Voltage degradation rate at 0.4 A cm$^{-2}$ (%/1000 h) (from the point of state 1) |
|---|---|---|---|---|
| State 1 | 0 | 1.10 | 0.88 | 0 |
| State 2 | 2300 | 1.10 | 0.92 | No degradation |
| State 3 | 3950 | 1.08 | 0.85 | 0.86 |
| State 4 | 5200 | 1.08 | 0.85 | 0.86 |
| State 5 | 5670 | 1.07 | 0.81 | 1.40 |
| State 6 | 6500 | 1.07 | – | – |

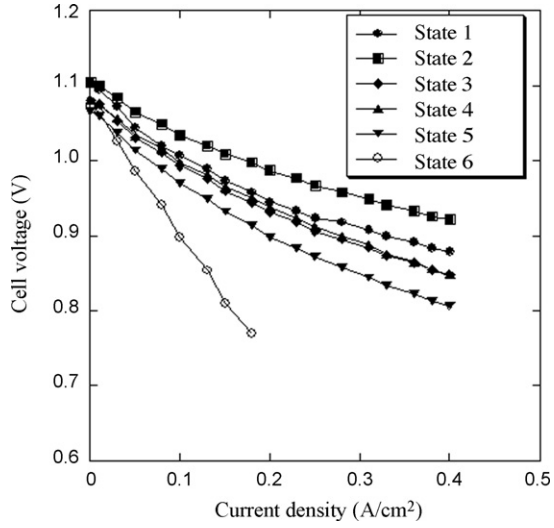


**Fig. 3.** Cell performance for each state.

high-frequency arc depends on the air condition (ratio of oxygen pressure, gas flow rate), while that for a low-frequency arc does not change, but depends on the hydrogen condition. Therefore, we estimated the resistances for cathode and anode polarizations from the high- and low-frequency arcs. The ohmic resistance, $R_0$, was also estimated. Curve fitting and resistance estimation were undertaken with ZView software. The data from the impedance measurements were analyzed with an equivalent circuit consisting of a resistance ($R$) and a constant phase element (CPE). Fig. 5 shows the resistances of the cell obtained from the impedance spectrum as a function of the operating time. The total cell resistance increases during the operating time. In particular, the cathode polarization resistance increases with operating time. The increase in the ohmic resistance along with that in the cathode polarization resistance constitutes the major reason for the voltage drop during operation. The ohmic resistance increased considerably after the second period of thermal cycling.

During the measurement, we found that the cathode exhaust gas contained $H_2O$ vapor. Basically, there should be no water on the cathode side. Since we observed water, we believe that the hydrogen anode gas leaked to the cathode side through a crack, and reacted with the cathode gas. The crack must have formed during the thermal cycles because the OCV gradually decreased after each one. Therefore, this suggests that the cathode polarization resistance increased owing to the presence of water in the cathode exhaust gas. It remains unclear why the ohmic resistance increased solely through the presence of water.

Moreover, we do not think that the cell itself was weak with respect to the thermal cycles, because we have already confirmed that there is little degradation in the $I$–$V$ characteristic of a cell with a metallic alloy housing (interconnects) during thermal cycling [18]. The alloy has a thermal expansion coefficient of $\sim 11.7 \times 10^{-6}\,K^{-1}$, which is close to that of the cell ($\sim 10.0 \times 10^{-6}\,K^{-1}$). In contrast, the value for alumina was $\sim 7.0 \times 10^{-6}\,K^{-1}$. Therefore, the observed crack could be caused by the difference between the thermal expansion coefficients of the alumina housing and the cell.

To investigate the factor contributing to the increase in the ohmic resistance, we used ICP to analyze the chemical composition of the water condensed in the cathode exhaust gas. We identified B and Si in the water and confirmed that these elements were from

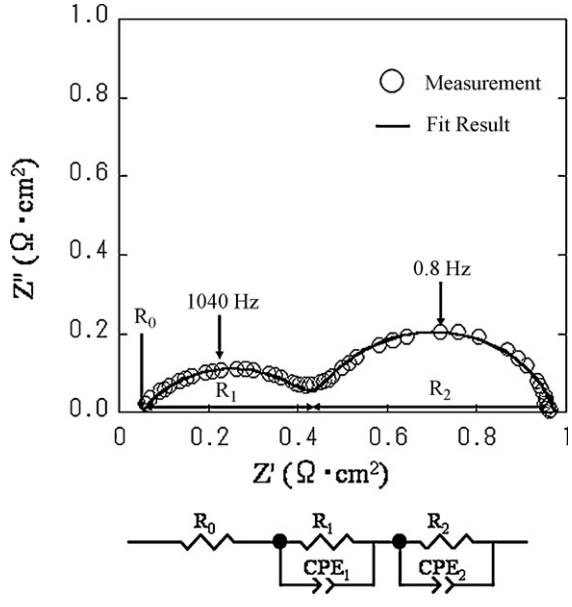


**Fig. 4.** Impedance spectrum for state 1.

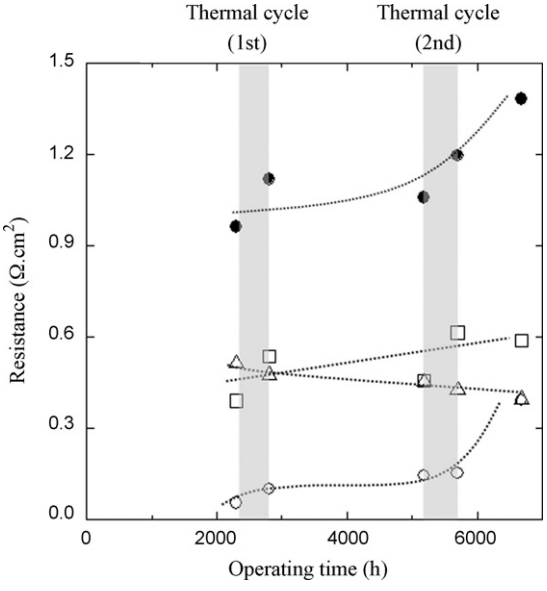


**Fig. 5.** Resistances from impedance spectra as a function of operating time: (○) ohmic resistance $R_0$; (□) cathode polarization resistance $R_1$; (△) anode polarization resistance $R_2$; (●) total resistance $R_{total}$.

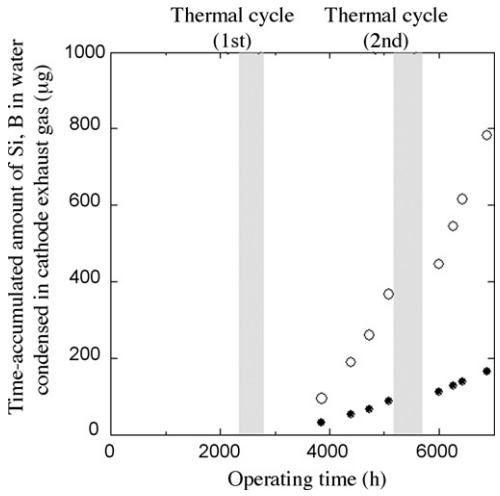


**Fig. 6.** Time-accumulated amount of Si (○) and B (●) in the water condensed in cathode exhaust gas.

the glass used as the sealant. This suggests that B and Si diffused from the sealant glass into the cathode gas. Fig. 6 shows the time-accumulated amount of B and Si obtained with the analysis. The time-accumulated amount of B and Si increased with time. We believe that Si and B diffused from the sealant glass. Because the leaks induced by the thermal cycles generated water, we were able to detect them. Therefore, there is the possibility that the cathode performance degrades owing to the reaction of elements such as B or Si that diffuse from the sealant glass. According to Horita et al., zirconia reacts with borosilicate glass at 1473 K and a new phase ZrSiCMs produced [19]. In our measurements, $ZrSiO_4$ might be formed by the reaction between the zirconia electrolyte and the vapor Si species scattered from the glass sealant. If $ZrSiO_4$ were formed, it would lead to enhanced ohmic resistance and cathodic resistance because the electronic conductivity of $ZrSiO_4$ is low. We think that the change in cell performance after thermal cycling is associated with the presence of $ZrSiO_4$.

From the various analyses, we found that several factors contribute to the increase in the ohmic resistance, including the elements (Si and B) from the sealant glass in the cathode exhaust gas. The dominant factor in the deterioration is still unclear.

## 4. Conclusion

Anode-supported cells with an LNF cathode were electrochemically characterized to investigate their long-term stability. A high current density was applied to the cell during operation for over 6500 h. We observed voltage degradation rates of 0.86%/1000 h (between 0 and 5200 h) and 1.40%/1000 h (between 0 and 5670 h) mainly due to the contact resistance between the cathode and electrolyte. The degradation was caused by increases in the cathode polarization resistance and ohmic resistance. During a long-term test, elements (Si and B) from the sealant glass were detected in water condensed in the cathode exhaust gas.

## References

[1] N.Q. Minh, T. Takahashi, Science and Technology of Ceramic Fuel Cells, Elsevier, Amsterdam, 1995.
[2] S.C. Singhal, K. Kendall, High-temperature Solid Oxide Fuel Cells: Fundamentals, Design and Applications, Elsevier Science, 2003.
[3] R. Chiba, F. Yoshimura, Y. Sakurai, Solid State Ionics 124 (1999) 281–288.
[4] T. Komatsu, H. Arai, R. Chiba, K. Nozawa, M. Arakawa, K. Sato, Electrochem. Solid-State Lett. 9 (2006) A9–A12.
[5] T. Komatsu, H. Arai, R. Chiba, K. Nozawa, M. Arakawa, K. Sato, J. Electrochem. Soc. 154 (2007) B379–B382.
[6] T. Komatsu, R. Chiba, H. Arai, K. Sato, J. Power Sources 176 (2008) 132–137.
[7] H. Orui, K. Watanabe, R. Chiba, M. Arakawa, J. Electrochem. Soc. 151 (2004) A1412.
[8] H. Orui, K. Nozawa, K. Watanabe, S. Sugita, R. Chiba, T. Komatsu, H. Arai, M. Arakawa, J. Electrochem. Soc. 155 (2008) B1100–B1116.
[9] M. Yokoo, Y. Tabata, Y. Yoshida, K. Hayashi, Y. Nozaki, K. Nozawa, H. Arai, J. Power Sources 178 (2008) 59–63.
[10] M. Yokoo, Y. Tabata, Y. Yoshida, H. Orui, K. Hayashi, Y. Nozaki, K. Nozawa, H. Arai, J. Power Sources 184 (2008) 84–89.
[11] T. Inagaki, F. Nishiwaki, S. Yamasaki, T. Akbay, K. Hosoi, J. Power Sources 181 (2008) 274–280.
[12] K. Fujita, T. Somekawa, K. Horiuchi, Y Matsuzaki, J. Power Sources, in press.
[13] T. Horita, H. Kishimoto, K. Yamaji, M.E. Brito, Y. Xiong, H. Yokokawa, Y. Hori, I. Miyachi, J. Power Sources, in press.
[14] K. Haga, S. Adachi, Y. Shiratori, K. Itoh, K. Sasaki, Solid State Ionics 179 (2008) 1427–1431.
[15] K. Nozawa, H. Orui, R. Chiba, M. Arakawa, in: H. Yokokawa, S.C. Singhal (Eds.), Solid Oxide Fuel Cells VII, PV 2001-16, The Electrochemical Society Proceedings Series, Pennington, NJ, 2001, p. 983.
[16] R. Chiba, Y. Tabata, T. Komatsu, H. Orui, K. Nozawa, M. Arakawa, H. Arai, Solid State Ionics 178 (2008) 1701–1709.
[17] R. Chiba, H. Orui, T. Komatsu, Y. Tabata, K. Nozawa, M. Arakawa, K. Sato, H. Arai, J. Electrochem. Soc. 155 (2008) B575–B580.
[18] T. Komatsu, S. Sugita, H. Arai, private communication.
[19] T. Horita, N. Sasaki, T. Kawada, H. Yokokawa, M. Dokiya, Denki Kagaku 61 (1993) 760–762.